Al(1)	24 (*l*)	0.2341 (4)	0.3952 (4)	0.1635 (2)	0.009 (1)
Al(2)	12 (*k*)	0.1560 (5)	0	0.1149 (3)	0.011 (2)
Al(3)	12 (*k*)	0.2529 (5)	0	0.5289 (3)	0.009 (2)
Al(4)	12 (*j*)	0.1481 (6)	0.5472 (6)	1/4	0.010 (2)
Al(5)	12 (*i*)	0.2495 (3)	2*x*	0	0.029 (2)
Al(6)†	8 (*h*)	1/3	2/3	0.1313 (2)	0.010 (1)
Al(7)	6 (g)	0.8498 (7)	0	1/4	0.006 (2)

† Al(6) site occupied by 44 (2)% Cr; set isotropic.

Table 2. *Interatomic distances* (<4 Å)

Yb—Al(4)	×2	3.044 (6)	Al(2)—Al(7)	×2	2.897 (6)
Yb—Al(5)	×2	3.057 (5)	Al(2)—Al(2)	×2	2.936 (7)
Yb—Al(1)	×2	3.062 (4)	Al(2)—Yb		3.389 (4)
Yb—Al(3)		3.190 (4)	Al(2)—Al(5)	×2	3.900 (8)
Yb—Al(6)	×2	3.219 (1)	Al(3)—Al(2)		2.737 (6)
Yb—Al(1)	×2	3.232 (8)	Al(3)—Al(5)	×2	2.740 (9)
Yb—Al(3)		3.270 (4)	Al(3)—Cr(2)		2.795 (8)
Yb—Al(5)	×2	3.369 (5)	Al(3)—Al(2)	×2	2.837 (11)
Yb—Al(2)		3.389 (4)	Al(3)—Al(1)	×2	2.885 (6)
Yb—Yb		3.444 (1)	Al(3)—Al(3)	×2	2.930 (12)
Yb—Cr(1)		3.498 (2)	Al(3)—Yb		3.190 (4)
Cr(1)—Al(7)	×2	2.478 (4)	Al(3)—Yb		3.270 (4)
Cr(1)—Al(2)	×2	2.638 (5)	Al(4)—Cr(1)		2.681 (6)
Cr(1)—Al(1)	×4	2.681 (8)	Al(4)—Al(1)	×2	2.730 (14)
Cr(1)—Al(4)	×2	2.681 (6)	Al(4)—Al(6)	×2	2.732 (12)
Cr(1)—Yb	×2	3.498 (2)	Al(4)—Al(1)	×2	2.764 (6)
Cr(2)—Al(2)	×6	2.635 (6)	Al(4)—Al(4)		2.787 (17)
Cr(2)—Al(3)	×6	2.795 (8)	Al(4)—Yb	×2	3.044 (6)
Al(1)—Al(6)		2.647 (8)	Al(4)—Al(4)	×2	3.062 (24)
Al(1)—Cr(1)		2.681 (8)	Al(5)—Al(5)	×2	2.734 (13)
Al(1)—Al(2)		2.709 (8)	Al(5)—Al(3)	×2	2.740 (9)
Al(1)—Al(4)		2.730 (14)	Al(5)—Al(6)	×2	2.794 (6)
Al(1)—Al(4)		2.764 (6)	Al(5)—Yb	×2	3.057 (5)
Al(1)—Al(7)		2.792 (9)	Al(5)—Al(1)	×2	3.057 (4)
Al(1)—Al(3)		2.885 (6)	Al(5)—Yb	×2	3.369 (5)
Al(1)—Al(1)		3.032 (7)	Al(5)—Al(2)	×2	3.900 (8)
Al(1)—Al(1)		3.038 (4)	Al(6)—Al(1)	×3	2.647 (8)
Al(1)—Al(5)		3.057 (4)	Al(6)—Al(4)	×3	2.732 (12)
Al(1)—Yb		3.062 (4)	Al(6)—Al(5)	×3	2.794 (6)
Al(1)—Yb		3.232 (8)	Al(6)—Yb	×3	3.219 (1)
Al(2)—Cr(2)		2.635 (6)	Al(7)—Cr(1)	×2	2.478 (4)
Al(2)—Cr(1)		2.638 (5)	Al(7)—Al(1)	×4	2.792 (9)
Al(2)—Al(1)	×2	2.709 (8)	Al(7)—Al(7)	×2	2.827 (9)
Al(2)—Al(3)		2.737 (6)	Al(7)—Al(2)	×4	2.897 (6)
Al(2)—Al(3)	×2	2.837 (11)			

The structure was solved by *MULTAN*87 (Debaerdemaeker, Germain, Main, Tate & Woolfson, 1987) and refined by least-squares techniques varying the scale factor, isotropic extinction, atomic positional and anisotropic displacement parameters. The Al(6) site, about half occupied by Cr, was set isotropic and its occupancy parameter was refined. *Xtal*3.2 (Hall, Flack & Stewart, 1992) was used for the data reduction and structure refinement. The high value of the displacement parameter of the Al(5) site has been noted. Refinement of the occupancy and displacement parameters of the Al(5) site did not improve the results.

Lists of structure factors and anisotropic displacement parameters have been deposited with the IUCr (Reference: DU1079). Copies may be obtained through The Managing Editor, International Union of Crystallography, 5 Abbey Square, Chester CH1 2HU, England.

References

Blanc, E., Schwarzenbach, D. & Flack, H. D. (1991). *J. Appl. Cryst.* **24**, 1035–1041.

Debaerdemaeker, T., Germain, G., Main, P., Tate, C. & Woolfson, M. M. (1987). *MULTAN*87. *A System of Computer Programs for the Automatic Solution of Crystal Structures from X-ray Diffraction Data*. Univs. of York, England, and Louvain, Belgium.

Hall, S. R., Flack, H. D. & Stewart, J. M. (1992). Editors. *Xtal*3.2. *Users Manual*. Univs. of Western Australia, Australia, Geneva, Switzerland, and Maryland, USA.

Kripyakevich, P. I. (1977). *Structure Types of Intermetallic Compounds*, pp. 92–99. Moscow: Nauka.

Rykhal', R. M., Zarechnyuk, O. S. & Mats'kiv, O. P. (1979). *Vestn. L'viv Univ. Ser. Khim.* **21**, 46–49.

Schubert, K. (1964). *Kristallstrukturen zweikomponentiger Phasen*, pp. 294–295. Berlin: Springer-Verlag.

Smith, J. F. & Ray, A. E. (1957). *Acta Cryst.* **10**, 169–172.

Zachariasen, W. H. (1968). *Acta Cryst.* A**24**, 212–216.

Zarechnyuk, O. S., Rykhal', R. M. & German, N. V. (1971). *Visn. L'viv Univ. Ser. Khim.* **12**, 10–12.

Zarechnyuk, O. S., Yanson, T. I., Ostrovskaya, O. I. & Shevchuk, L. P. (1988). *Visn. L'viv Univ. Ser. Khim.* **29**, 44–47.

Acta Cryst. (1994). C**50**, 1531–1536

Rietveld Refinement of the Structures of Dry-Synthesized MFe^{III}Si$_2$O$_6$ Leucites (M = K, Rb, Cs) by Synchrotron X-ray Powder Diffraction

A. M. T. Bell

SERC Daresbury Laboratory, Daresbury, Warrington, Cheshire WA4 4AD, England

C. M. B. Henderson

Department of Geology, University of Manchester, Manchester M13 9PL, England

(*Received* 25 *January* 1994; *accepted* 13 *April* 1994)

Abstract

Analyses of high-resolution synchrotron X-ray powder diffraction patterns of dry-synthesized MFe^{III}Si$_2$O$_6$ leucites (M = K, Rb, Cs) showed that the K- and Rb-containing leucites (iron potassium silicate, KFeSi$_2$O$_6$, and iron rubidium silicate, RbFeSi$_2$O$_6$) each have a tetragonal $I4_1/a$ structure and the Cs-containing leucite (caesium iron silicate, CsFeSi$_2$O$_6$) has a cubic $Ia\bar{3}d$ structure. The structures of these materials have been refined by the Rietveld method. In CsFeSi$_2$O$_6$ leucite, Fe^{III} and Si are disordered on tetrahedral framework sites as required by space-group constraints. In KFeSi$_2$O$_6$ leucite, Fe shows significant ordering and is concentrated on the T_3 tetrahedral site. RbFeSi$_2$O$_6$ leucite shows less pronounced T-site ordering reflecting the fact that it is closer to the tetragonal–cubic phase transition at which the T sites become identical.

Comment

As part of a wider attempt to understand the controls and consequences of tetrahedral-site cation ordering in compounds with framework structures, we are studying a series of synthetic silicates with structures related to that of natural leucite ($KAlSi_2O_6$). Many of these materials have framework cation species that are more amenable to tetrahedral-site (*T*-site) analysis than their Al/Si analogues, and also display different *T*-site ordering arrangements depending on the conditions of their synthesis and on their chemical compositions (Bell, Henderson, Redfern, Cernik, Champness, Fitch & Kohn, 1994*a*; Bell, Redfern, Henderson & Kohn, 1994*b*).

The structure of leucite consists of a three-dimensional framework of interconnected SiO_4 and AlO_4 tetrahedra with K^+ ions occupying channels within the framework. Other phases having the leucite structure include the natural minerals pollucite ($CsAlSi_2O_6$) and analcime ($NaAlSi_2O_6.H_2O$) and a wide variety of synthetic materials with different stoichiometries (for a review see Kohn, Dupree, Mortuza & Henderson, 1991) and which crystallize in different space groups (Torres-Martinez & West, 1989; Bell, Cernik, Champness, Fitch, Henderson, Kohn, Norledge & Redfern, 1993; Bell *et al.*, 1994*a*,*b*). All of these phases have the same topology with the different space groups being related by reversible displacive transitions and different tetrahedral-site ordering patterns. Thus natural leucite ($KAlSi_2O_6$) has a tetragonal $I4_1/a$ structure with Al and Si distributed over three separate tetrahedral (*T*) sites (denoted T_1, T_2 and T_3) (Mazzi, Galli & Gottardi, 1976) while pollucite ($CsAlSi_2O_6$) is cubic $Ia\bar{3}d$ with Si and Al disordered over a single *T* site (Beger, 1969). $KAlSi_2O_6$ leucite transforms rapidly and reversibly to a metrically cubic structure at high temperature. This high-temperature leucite was originally believed to be cubic $Ia\bar{3}d$ (Peacor, 1968), leading to the conclusion that in the low-temperature form Si and Al were fully disordered over the three *T* sites. Recent magic-angle-spinning NMR work has, however, shown that natural leucite shows partial *T*-site ordering, although different ordering arrangements have been proposed (Brown, Cardile, MacKenzie, Ryan & Meinhold, 1987; Murdoch, Stebbins, Carmichael & Pines, 1988; Phillips, Kirkpatrick & Putnis, 1989; Kohn, Henderson & Dupree, 1994). Taylor & Henderson (1968) studied the thermal expansion of a natural leucite and synthetic samples having the stoichiometry $MAlSi_2O_6$, with M = K, Rb and Cs, and noted that tetragonal $RbAlSi_2O_6$ also showed a displacive transition to a cubic $Ia\bar{3}d$ structure at high temperature.

Several workers have studied synthetic leucites with the stoichiometry $MFe^{III}Si_2O_6$ in which Fe^{III} substitutes for Al in the tetrahedral sites. Faust (1963) showed that the X-ray powder diffraction pattern of the K,Fe compound could be indexed as tetragonal $I4_1/a$ and that this material underwent a phase transition at high temperature similar to that for $KAlSi_2O_6$ leucite. Hirao, Soga & Masanaga (1976) found that $KFeSi_2O_6$, $RbFeSi_2O_6$, $(Rb_{0.9}Cs_{0.1})FeSi_2O_6$ and $(Rb_{0.8}Cs_{0.2})FeSi_2O_6$ leucites all showed tetragonal–cubic phase transitions at high temperatures. Kopp, Harris, Clark & Lakel (1963) used the relative intensities of peaks in an X-ray powder diffraction pattern to deduce that synthetic $CsFeSi_2O_6$ leucite is cubic $Ia\bar{3}d$ at room temperature; this space group has a single *T* site and so requires a disordered tetrahedral-site cation arrangement. However, Faust (1963) and Lange, Carmichael & Stebbins (1986) suggested that $KFeSi_2O_6$ leucite might contain an ordered arrangement of Fe^{III} and Si. Brown *et al.* (1987) studied $KFeSi_2O_6$ leucite by ^{57}Fe Mössbauer spectroscopy and fitted three doublets to the spectrum obtained. By assigning the doublets with the higher quadrupole splittings to the more distorted *T* sites (order of distortion $T_1 > T_2 > T_3$), they determined site occupancies for Fe of T_1 0.19, T_2 0.34 and T_3 0.47. In a recent Mössbauer study of synthetic Fe leucites, England, Henderson, Charnock & Vaughan (1994) found similar values of 0.12, 0.35 and 0.52, respectively, for $KFeSi_2O_6$ leucite, while the Mössbauer spectrum of $CsFeSi_2O_6$ showed a broad doublet, reflecting the wide range of local environments for Fe in the cubic $Ia\bar{3}d$ structure in which Fe and Si are disordered over a single *T* site.

Although structural relationships for *M*,Fe leucites have been deduced in previous work, no structures have been determined directly. In the present paper we describe the structures of three dry-synthesized leucites with the stoichiometry $MFe^{III}Si_2O_6$, where M = K, Rb, Cs, determined using X-ray powder diffraction techniques and Rietveld analysis (Rietveld, 1969). Observed, calculated and difference profiles for the K, Rb and Cs Fe^{III} leucites are shown in Figs. 1, 2 and 3, respectively. The difference plots for the K- and Cs-containing compounds show that the agreement between the observed and calculated profiles is good, but the fit for $RbFeSi_2O_6$ is less good as a consequence of some [001] preferred orientation in the sample.

The refined *T*—O distances for $KFeSi_2O_6$ leucite decrease in the order $T_3 > T_2 > T_1$; these values represent weighted averages for Si—O and Fe^{III}—O distances for each *T* site. The mean *T*—O distances for the three *T* sites can be used to calculate the site occupancies based on tetrahedral bond lengths of 1.86 Å for Fe^{III}—O and 1.60 Å for Si—O. The values obtained for the Fe occupancies using this method are T_1 0.28, T_2 0.30 and T_3 0.42. These values may be compared with the refined site occupancies of 0.29 (1), 0.35 (1) and 0.36 (1). Mazzi *et al.* (1976) found that for natural leucite the order of decreasing *T*-site distortion is $T_1 > T_2 > T_3$; the relative distortions can be assessed using the tetrahedral angle variances σ^2 (in degrees^2) (Robinson,

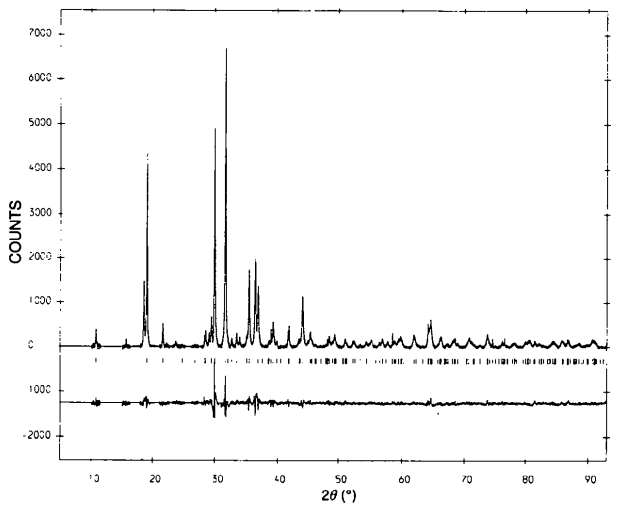

Fig. 1. Rietveld difference plot for dry-synthesized $KFeSi_2O_6$.

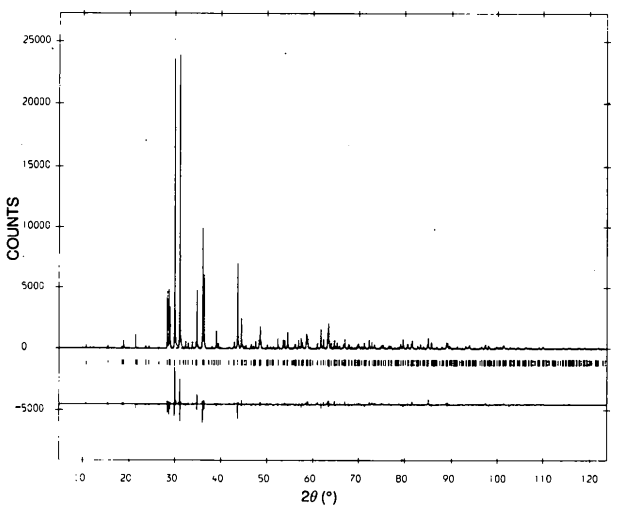

Fig. 2. Rietveld difference plot for dry-synthesized $RbFeSi_2O_6$.

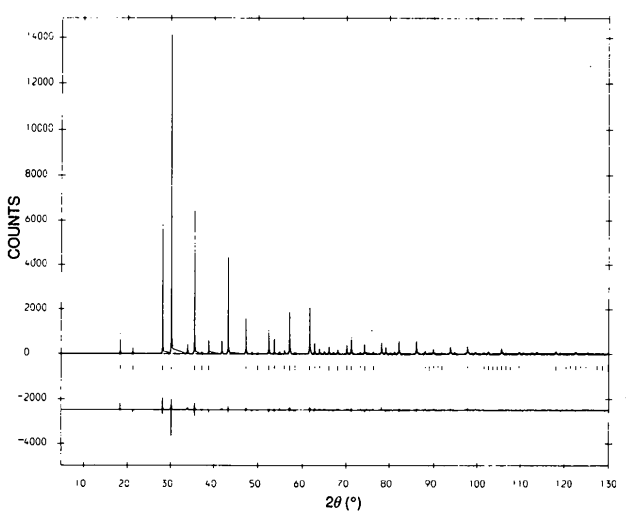

Fig. 3. Rietveld difference plot for dry-synthesized $CsFeSi_2O_6$.

Gibbs & Ribbe, 1971) of 8.7, 5.4 and 2.3, respectively. As expected, the angle variances for the Fe leucites studied here are considerably higher as a result of the presence of the larger Fe cations in the framework. Angle variances for $KFeSi_2O_6$ leucite are T_1 8.7, T_2 13.3 and T_3 28.0; thus Fe seems to be preferentially ordered into the most distorted T site, confirming the Mössbauer site assignments of Brown *et al.* (1987) and England *et al.* (1994). Note that these Fe leucites do not show the same relative distortions for the three T sites as natural leucite (Mazzi *et al.*, 1976), suggesting that Al and Fe have significantly different effects on the geometries of the TO_4 tetrahedra.

The tetrahedral angle variances in $RbFeSi_2O_6$ leucite are larger than those in $KFeSi_2O_6$ (T_1 30.6, T_2 23.1 and T_3 57.9); the T_3 site is again the most distorted. The mean T—O distances decrease in the order $T_3 > T_2 \simeq T_1$ leading to values for the Fe occupancies of T_1 0.31, T_2 0.27 and T_3 0.42. These values may be compared with those obtained from the Rietveld refinement: 0.31 (1), 0.36 (1) and 0.33 (1), respectively. The occupancies calculated from the bond lengths might be the more reliable as the R factor for the refinement in which the possibility of ordering was included was little better than that for the refinement in which disorder was assumed. In addition, the model for the $RbFeSi_2O_6$ leucite structure is slightly less reliable than for the other two leucites because of preferred orientation in the sample. In $RbFeSi_2O_6$ leucite, therefore, Fe seems to be slightly ordered into the most distorted T site (T_3) but the degree of ordering is less than that in $KFeSi_2O_6$ leucite. $RbFeSi_2O_6$ leucite is less tetragonal than $KFeSi_2O_6$ leucite (c/a = 1.036 and 1.055, respectively) with a lower tetragonal–cubic transition temperature [593 and 843 K, respectively (Hirao *et al.*, 1976)]. The differences between the local geometries of the three T sites decrease as temperature or mean size of the alkali-metal cations in the cavities increases and thus less T-site ordering might be expected in Rb leucites than in K leucites.

For the cubic $Ia\bar{3}d$ $CsFeSi_2O_6$ leucite the refined T—O distance represents the weighted average of tetrahedral Si—O and Fe^{III}—O distances. The tetrahedral angle variance for the single T site is 47.3; this value compares well with the mean for the three T sites in $RbFeSi_2O_6$ leucite. The displacement factors for the framework components in $CsFeSi_2O_6$ leucite are larger than those for the $KFeSi_2O_6$ and $RbFeSi_2O_6$ leucites as a result of the more disordered nature of the structure. As might be expected, the alkali-metal cation displacement factors vary inversely with cation size.

Taylor & Henderson (1968) discussed the thermal expansion and tetragonal–cubic phase-transition behaviour of K, Rb and Cs aluminosilicate leucites in terms of collapse of the framework about the cavity cations. Decreasing temperature and decreasing mean cavity cation

size lead to structures that are more collapsed, as a cooperative rotation of the TO_4 units to form stronger bonds with the alkali-metal cations occurs. Hirao *et al.* (1976) used this same explanation to account for the behaviour of the analogous alkali-metal ferro-silicate leucites. The structures determined in this paper confirm these relationships as the mean T—O—T angles decrease with decreasing alkali-metal cation size (Cs 140.1, Rb 135.3, K 135.0°). Note that the T—O—T angles tend to increase as framework structures become more symmetrical, *i.e.* less collapsed.

Comparison of the projections of the structures of $KFeSi_2O_6$ and $CsFeSi_2O_6$ in Figs. 4 and 5, respectively, shows how the channels in the framework become distorted as the structure collapses. The structure of $RbFeSi_2O_6$ is similar to that of $KFeSi_2O_6$, but has slightly less distorted channels.

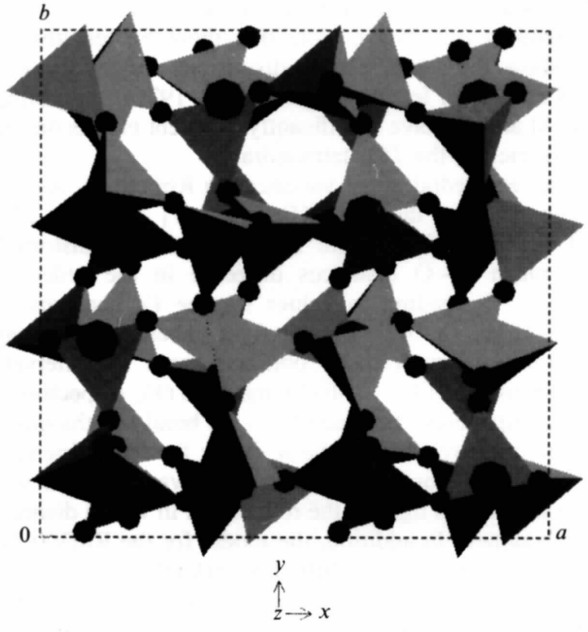

Fig. 4. A projection of the structure of $KFeSi_2O_6$ along [001]. Tetrahedra represent TO_4 units, large circles represent K^+ cations and small circles represent O^{2-} anions.

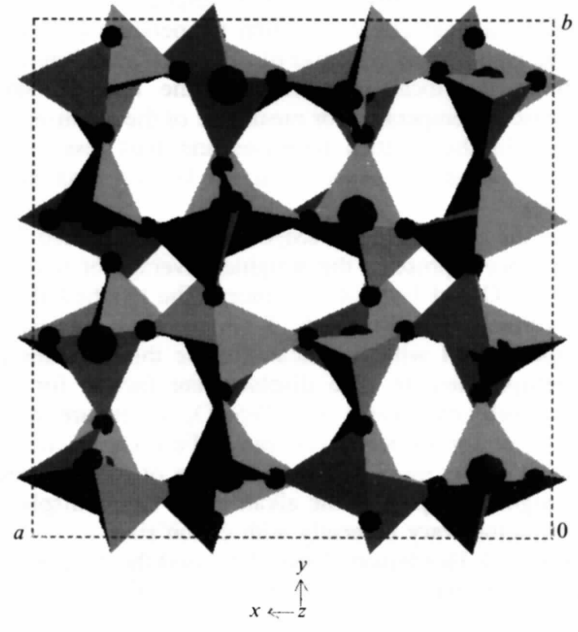

Fig. 5. A projection of the structure of $CsFeSi_2O_6$ along [001]. Tetrahedra represent TO_4 units, large circles represent Cs^+ cations and small circles represent O^{2-} anions.

Experimental

Appropriate proportions of the relevant alkali-metal carbonate, Fe_2O_3 and SiO_2 were ground together to provide the starting materials. The K-containing mix was melted at 1523 K for two days and was quenched to form a glass, followed by crystallization at 1073 K for four days. The Rb- and Cs-containing mixes were recrystallized at 1673 K for three days.

$KFeSi_2O_6$

Crystal data

$KFeSi_2O_6$
M_r = 247.11
Tetragonal
$I4_1/a$
a = 13.2207 (3) Å
c = 13.9464 (3) Å
V = 2437.6 (2) Å^3
Z = 16

Synchrotron radiation
λ = 1.80067 Å
T = 293 K
Powder
Sample mounted in reflection mode

Data collection

High resolution powder diffractometer, SRS station 8.3 (Cernik, Murray, Pattison & Fitch, 1990)
Parallel beam non-focusing optics with channel-cut monochromator and scintillation detector

Method for scanning reciprocal space: step scan
Absorption correction method: none
8800 data points measured
8800 data points in the processed diffractogram
$2\theta_{min}$ = 5.00, $2\theta_{max}$ = 92.99°
Increment in 2θ = 0.01°

Refinement

R_I = 0.045 (Young, Prince & Sparks, 1982)
R_{wp} = 0.154 (Young, Prince & Sparks, 1982)
R_{exp} = 0.120 (Young, 1993)
S = 1.645
352 reflections

50 parameters
Atomic scattering factors from *International Tables for X-ray Crystallography* (1974, Vol. IV, Table 2.3.1)

Table 1. *Fractional atomic coordinates, isotropic displacement parameters* (Å^2) *and site occupancy factors for* $KFeSi_2O_6$

	x	y	z	B_{iso}	Occupancy
K	0.3620 (5)	0.3641 (4)	0.1174 (5)	4.9 (2)	1.00
Si1	0.0570 (4)	0.3972 (4)	0.1643 (4)	0.87 (9)	0.71 (1)
Si2	0.1649 (4)	0.6130 (4)	0.1271 (4)	0.87 (9)	0.65 (1)
Si3	0.3914 (4)	0.6440 (4)	0.0851 (3)	0.87 (9)	0.64 (1)

Fe1	0.0570 (4)	0.3972 (4)	0.1643 (4)	0.87 (9)	0.29 (1)
Fe2	0.1649 (4)	0.6130 (4)	0.1271 (4)	0.87 (9)	0.35 (1)
Fe3	0.3914 (4)	0.6440 (4)	0.0851 (3)	0.87 (9)	0.36 (1)
O1	0.1299 (9)	0.3181 (9)	0.1165 (7)	0.25	1.00
O2	0.0890 (8)	0.5125 (9)	0.1322 (8)	0.25	1.00
O3	0.1486 (8)	0.6787 (7)	0.2299 (8)	0.25	1.00
O4	0.1279 (9)	0.6823 (7)	0.0382 (8)	0.25	1.00
O5	0.2885 (9)	0.5727 (8)	0.125 (1)	0.25	1.00
O6	0.4818 (8)	0.6131 (7)	0.1758 (7)	0.25	1.00

Table 2. *Selected geometric parameters* (Å, °) *for* $KFeSi_2O_6$

T represents Si or Fe.

*T*1—O1	1.57 (1)	*T*3—O5	1.75 (1)
*T*1—O1′	1.72 (1)	*T*3—O6	1.79 (1)
*T*1—O2	1.64 (1)	*T*3—O6′	1.69 (1)
*T*1—O4	1.75 (1)	K—O1	3.13 (1)
*T*2—O2	1.67 (1)	K—O2	2.99 (1)
*T*2—O3	1.69 (1)	K—O3	3.11 (1)
*T*2—O4′	1.62 (1)	K—O4	3.03 (1)
*T*2—O5	1.72 (1)	K—O5	2.93 (1)
*T*3—O3′	1.65 (1)	K—O6	2.96 (1)
O1—*T*1—O1′	113.2 (6)	O3′—*T*3—O5	109.4 (6)
O1—*T*1—O2	110.2 (6)	O3′—*T*3—O6	110.6 (5)
O1—*T*1—O4	105.8 (6)	O3′—*T*3—O6′	108.6 (6)
O1′—*T*1—O2	107.6 (6)	O5—*T*3—O6	99.9 (6)
O1′—*T*1—O4	107.7 (6)	O5—*T*3—O6′	112.4 (6)
O2—*T*1—O4	112.5 (6)	O6—*T*3—O6′	115.6 (6)
O2—*T*2—O3	107.3 (6)	*T*1—O1—*T*1	145.7 (8)
O2—*T*2—O4′	107.6 (6)	*T*1—O2—*T*2	154.9 (7)
O2—*T*2—O5	109.0 (5)	*T*2—O3—*T*3	130.2 (6)
O3—*T*2—O4′	108.7 (5)	*T*1—O4—*T*2	139.3 (7)
O3—*T*2—O5	107.2 (6)	*T*2—O5—*T*3	125.4 (7)
O4′—*T*2—O5	116.7 (6)	*T*3—O6—*T*3	122.4 (6)

$RbFeSi_2O_6$

Crystal data

$RbFeSi_2O_6$
M_r = 293.48
Tetragonal
$I4_1/a$
a = 13.4586 (1) Å
c = 13.9380 (1) Å
V = 2524.63 (5) Å^3
Z = 16

Synchrotron radiation
λ = 1.80067 Å
T = 293 K
Powder
Sample mounted in reflection mode

Data collection

High resolution powder diffractometer, SRS station 8.3 (Cernik, Murray, Pattison & Fitch, 1990)
Parallel beam non-focusing optics with channel-cut monochromator and scintillation detector

Method for scanning reciprocal space: step scan
Absorption correction method: none
11 876 data points measured
11 876 data points in the processed diffractogram
$2\theta_{min}$ = 5.00, $2\theta_{max}$ = 123.75°
Increment in 2θ = 0.01°

Refinement

R_I = 0.089 (Young, Prince & Sparks, 1982)
R_{wp} = 0.174 (Young, Prince & Sparks, 1982)
R_{exp} = 0.102 (Young, 1993)
S = 2.898
626 reflections

43 parameters
Atomic scattering factors from *International Tables for X-ray Crystallography* (1974, Vol. IV, Table 2.3.1)

Table 3. *Fractional atomic coordinates, isotropic displacement parameters* (Å^2) *and site occupancy factors for* $RbFeSi_2O_6$

	x	*y*	*z*	B_{iso}	Occupancy
Rb	0.3655 (2)	0.3632 (2)	0.1213 (2)	4.51 (7)	1.00
Si1	0.0645 (4)	0.3937 (4)	0.1629 (3)	2.62 (9)	0.69 (1)
Si2	0.1685 (4)	0.6062 (4)	0.1272 (4)	2.62 (9)	0.64 (1)
Si3	0.3883 (4)	0.6473 (4)	0.0885 (4)	2.62 (9)	0.67 (1)
Fe1	0.0645 (4)	0.3937 (4)	0.1629 (3)	2.62 (9)	0.31 (1)
Fe2	0.1685 (4)	0.6062 (4)	0.1272 (4)	2.62 (9)	0.36 (1)
Fe3	0.3883 (4)	0.6473 (4)	0.0885 (4)	2.62 (9)	0.33 (1)
O1	0.136 (1)	0.3122 (8)	0.1040 (8)	3.0 (1)	1.00
O2	0.0959 (9)	0.5032 (9)	0.1227 (7)	3.0 (1)	1.00
O3	0.1463 (9)	0.6690 (7)	0.2226 (8)	3.0 (1)	1.00
O4	0.1332 (9)	0.6734 (7)	0.0357 (8)	3.0 (1)	1.00
O5	0.2911 (9)	0.559 (1)	0.1236 (9)	3.0 (1)	1.00
O6	0.4795 (9)	0.6110 (9)	0.1563 (9)	3.0 (1)	1.00

Table 4. *Selected geometric parameters* (Å, °) *for* $RbFeSi_2O_6$

T represents Si or Fe.

*T*1—O1	1.67 (1)	*T*3—O5	1.83 (1)
*T*1—O1′	1.72 (1)	*T*3—O6	1.62 (1)
*T*1—O2	1.63 (1)	*T*3—O6′	1.70 (1)
*T*1—O4	1.73 (1)	Rb—O1	3.18 (1)
*T*2—O2	1.70 (1)	Rb—O2	3.20 (1)
*T*2—O3	1.60 (1)	Rb—O3	3.21 (1)
*T*2—O4′	1.63 (1)	Rb—O4	3.13 (1)
*T*2—O5	1.77 (1)	Rb—O5	2.82 (1)
*T*3—O3′	1.77 (1)	Rb—O6	3.25 (1)
O1—*T*1—O1′	117.3 (5)	O3′—*T*3—O5	101.3 (5)
O1—*T*1—O2	106.0 (6)	O3′—*T*3—O6	104.9 (6)
O1—*T*1—O4	112.3 (6)	O3′—*T*3—O6′	114.3 (6)
O1′—*T*1—O2	105.4 (6)	O5—*T*3—O6	101.0 (6)
O1′—*T*1—O4	102.9 (6)	O5—*T*3—O6′	117.8 (6)
O2—*T*1—O4	112.9 (6)	O6—*T*3—O6′	115.6 (7)
O2—*T*2—O3	110.7 (6)	*T*1—O1—*T*1	138.7 (8)
O2—*T*2—O4′	104.9 (6)	*T*1—O2—*T*2	150.9 (8)
O2—*T*2—O5	104.2 (5)	*T*2—O3—*T*3	134.2 (7)
O3—*T*2—O4′	107.5 (6)	*T*1—O4—*T*2	143.4 (7)
O3—*T*2—O5	112.7 (5)	*T*2—O5—*T*3	116.3 (8)
O4′—*T*2—O5	116.6 (5)	*T*3—O6—*T*3	134.2 (8)

$CsFeSi_2O_6$

Crystal data

$CsFeSi_2O_6$
M_r = 340.92
Cubic
$Ia\bar{3}d$
a = 13.8542 (1) Å
V = 2653.98 (3) Å^3
Z = 16

Synchrotron radiation
λ = 1.80067 Å
T = 293 K
Powder
Sample mounted in reflection mode

Data collection

High resolution powder diffractometer, SRS station 8.3 (Cernik, Murray, Pattison & Fitch, 1990)
Parallel beam non-focusing optics with channel-cut monochromator and scintillation detector

Method for scanning reciprocal space: step scan
Absorption correction method: none
12 501 data points measured
12 501 data points in the processed diffractogram
$2\theta_{min}$ = 5.00, $2\theta_{max}$ = 130.00°
Increment in 2θ = 0.01°

Refinement

R_I = 0.106 (Young, Prince & Sparks, 1982)	15 parameters
R_{wp} = 0.173 (Young, Prince & Sparks, 1982)	Atomic scattering factors from *International Tables for X-ray Crystallography* (1974, Vol. IV, Table 2.3.1)
R_{exp} = 0.160 (Young, 1993)	
S = 1.171	
122 reflections	

Table 5. *Fractional atomic coordinates, isotropic displacement parameters* (Å^2) *and site occupancy factors for* $CsFeSi_2O_6$

	x	y	z	B_{iso}	Occupancy
Cs	1/8	1/8	1/8	3.10 (3)	1.00
Si	1/8	0.6628 (1)	0.5873 (1)	4.04 (6)	0.67
Fe	1/8	0.6628 (1)	0.5873 (1)	4.04 (6)	0.33
O	0.4686 (3)	0.3859 (3)	0.1509 (3)	4.5 (1)	1.00

Table 6. *Selected geometric parameters* (Å, °) *for* $CsFeSi_2O_6$

T represents Si or Fe.

T—O	× 2	1.706 (4)	Cs—O	× 6	3.573 (4)
T—O′	× 2	1.658 (4)	Cs—O′	× 6	3.365 (4)
O—*T*—O′	× 2	114.2 (2)	O′—*T*—O′		101.8 (2)
O′—*T*—O	× 2	113.8 (2)	*T*—O—*T*		140.1 (2)
O—*T*—O		99.7 (2)			

The systematic absences in the powder diffraction data for $KFeSi_2O_6$ and $RbFeSi_2O_6$ showed that these materials have the $I4_1/a$ leucite structure. Atomic coordinates from the low-temperature structure of natural leucite (Mazzi *et al.*, 1976) were used as a starting model for these refinements. The K compound contained a small but significant amount of haematite (Fe_2O_3) as an impurity. In this case, a two-phase refinement was performed using the structural parameters for haematite from Blake, Hessevick, Zoltai & Finger (1966). The systematic absences in the powder diffraction data for $CsFeSi_2O_6$ confirmed that this material has the cubic $Ia\bar{3}d$ structure, for which the atomic coordinates from the high-temperature structure of natural leucite (Peacor, 1968) were used as a starting model. The structures of the K- and Rb-containing leucites were initially refined in $I4_1/a$ assuming a disordered arrangement of Fe^{III} and Si on the tetrahedral sites, giving R_I factors of 0.064 and 0.097, respectively. In subsequent refinements the *T*-site occupancies were allowed to vary, leading to a significant improvement for $KFeSi_2O_6$ (R_I = 0.045) while $RbFeSi_2O_6$ showed a small improvement (R_I = 0.089). Data collection was performed using in-house software. The raw synchrotron powder diffraction data were normalized to account for the decay of the synchrotron radiation beam. Cell refinement was performed using *REFCEL* from the *Powder Diffraction Program Library* (*PDPL*) (Murray, Cockcroft & Fitch, 1990). Structure refinement was carried out using the program *MPROF* in *PDPL*. A pseudo-Voigt peak-shape function was used to model the shape of the Bragg peaks, and the least-squares weighting scheme used was weight = normalization factor/(profile intensity + background). Molecular graphics were prepared using *CERIUS* (Molecular Simulations Inc., 1994).

We acknowledge the use of the SERC-funded Chemical Database Service at Daresbury and also thank the SERC for award of synchrotron beamtime.

Lists of raw powder data have been deposited with the IUCr (Reference: BR1077). Copies may be obtained through The Managing Editor, International Union of Crystallography, 5 Abbey Square, Chester CH1 2HU, England.

References

Beger, R. M. (1969). *Z. Kristallogr.* **129**, 280–302.

Bell, A. M. T., Cernik, R. J., Champness, P. E., Fitch, A. N., Henderson, C. M. B., Kohn, S. C., Norledge, B. V. & Redfern, S. A. T. (1993). *Mater. Sci. Forum*, pp. 133–136, 697–702.

Bell, A. M. T., Henderson, C. M. B., Redfern, S. A. T., Cernik, R. J., Champness, P. E., Fitch, A. N. & Kohn, S. C. (1994*a*). *Acta Cryst.* B**50**, 31–41.

Bell, A. M. T., Redfern, S. A. T., Henderson, C. M. B. & Kohn, S. C. (1994*b*). *Acta Cryst.* B**50**. In the press.

Blake, R. L., Hessevick, R. E., Zoltai, T. & Finger, L. W. (1966). *Am. Mineral.* **51**, 123.

Brown, I. W. M., Cardile, C. M., MacKenzie, K. J. D., Ryan, M. J. & Meinhold, R. H. (1987). *Phys. Chem. Miner.* **15**, 78–83.

Cernik, R. J., Murray, P. K., Pattison, P. & Fitch, A. N. (1990). *J. Appl. Cryst.* **23**, 292–296.

England, K. E. R., Henderson, C. M. B., Charnock, J. M. & Vaughan, D. J. (1994). *Hyperfine Interactions*. In the press.

Faust, G. T. (1963). *Schweiz. Min. Petrogr. Mitt.* **43**, 165–195.

Hirao, K., Soga, N. & Masanaga, K. (1976). *J. Phys. Chem.* **80**, 1612–1616.

Kohn, S. C., Dupree, R., Mortuza, M. G. & Henderson, C. M. B. (1991). *Phys. Chem. Miner.* **18**, 144–152.

Kohn, S. C., Henderson, C. M. B. & Dupree, R. (1994). To be submitted to *Am. Mineral.*

Kopp, O. C., Harris, L. A., Clark, G. W. & Lakel, H. L. (1963). *Am. Mineral.* **48**, 100–109.

Lange, R. A., Carmichael, I. S. E. & Stebbins, J. F. (1986). *Am. Mineral.* **71**, 937–945.

Mazzi, F., Galli, E. & Gottardi, G. (1976). *Am. Mineral.* **61**, 108–115.

Molecular Simulations Inc. (1994). *CERIUS*. Molecular Simulations Inc., 240/250 The Quorum, Barnwell Road, Cambridge CB5 8RE, England.

Murdoch, J. B., Stebbins, J. F., Carmichael, I. S. E. & Pines, A. (1988). *Phys. Chem. Miner.* **15**, 370–382.

Murray, A. D., Cockcroft, J. K. & Fitch, A. N. (1990). *Powder Diffraction Program Library* (*PDPL*). University College, London.

Peacor, D. R. (1968). *Z. Kristallogr.* **127**, 213–224.

Phillips, B. L., Kirkpatrick, R. J. & Putnis, A. (1989). *Phys. Chem. Miner.* **16**, 262–275.

Rietveld, H. M. (1969). *J. Appl. Cryst.* **2**, 65–71.

Robinson, K., Gibbs, G. V. & Ribbe, P. H. (1971). *Science*, **172**, 567–570.

Taylor, D. & Henderson, C. M. B. (1968). *Am. Mineral.* **53**, 1476–1489.

Torres-Martinez, L. M. & West, A. R. (1989). *Z. Anorg. Allg. Chem.* **573**, 223–230.

Young, R. A. (1993). Editor. *The Rietveld Method*, p. 22. Oxford Univ. Press.

Young, R. A., Prince, E. & Sparks, R. A. (1982). *J. Appl. Cryst.* **15**, 357–359.